Electronic Supplementary Information

Principles on the electronic structure and optical response of heterobimetallic M-Dicyanoaurate-based coordination polymers (M = Mn, Co, Ni, Zn and Cd)

R. Mojica,[1,a] M. C. Vázquez,[a] A. E. Torres,[b] Y. Ávila,[a] R. Borja-Urby,[c] J. Rodríguez-Hernández,[d] and E. Reguera[2,a]

[a] *Centro de Investigación en Ciencia Aplicada y Tecnología Avanzada, Unidad Legaría, Instituto Politécnico Nacional, 11500, Miguel Hidalgo, Ciudad de México, México.*
[b] *Instituto de Ciencias Aplicadas y Tecnología, Universidad Nacional Autónoma de México, 04510, Coyoacán, Ciudad de México, México.*
[c] *Centro de Nanociencias y Micro y Nanotecnología, Instituto Politécnico Nacional, 07738, Gustavo A. Madero, Ciudad de México, México.*
[d] *Centro de Investigación en Química Aplicada, 25294, Saltillo, Coahuila, México.*

[1] Corresponding Author. Email: hmojicam1900@alumno.ipn.mx (R. Mojica) Tel: (+52) 55 5729 6000 Op. 67797
[2] Corresponding Author. Email: ereguerar@ipn.mx (E. Reguera) Tel: (+52) 55 5729 6000 Op. 67797

1 Experimental data

1.1 Experimental lattice parameters and Zn-DAu structure

In this section are presented the experimental results and data of M-DAu materials referred into the manuscript.

Lattice Parameters					
System	a(Å)	b(Å)	c(Å)	Volume(Å^3)	Au $\cdots$ Au(Å)
Co-DAu	6.82	6.82	7.80	315.25	3.33
Ni-DAu	6.84	6.84	7.68	312.08	3.33
Cd-DAu	6.86	6.86	8.21	335.19	3.17
Mn-DAu	6.85	6.85	8.02	326.03	3.27
Zn-DAu	8.42	8.42	20.84	1280.23	3.14/3.08
K-DAu	7.28	7.28	26.35	1209.86	3.64

Table 1: Lattice parameters of experimental structures

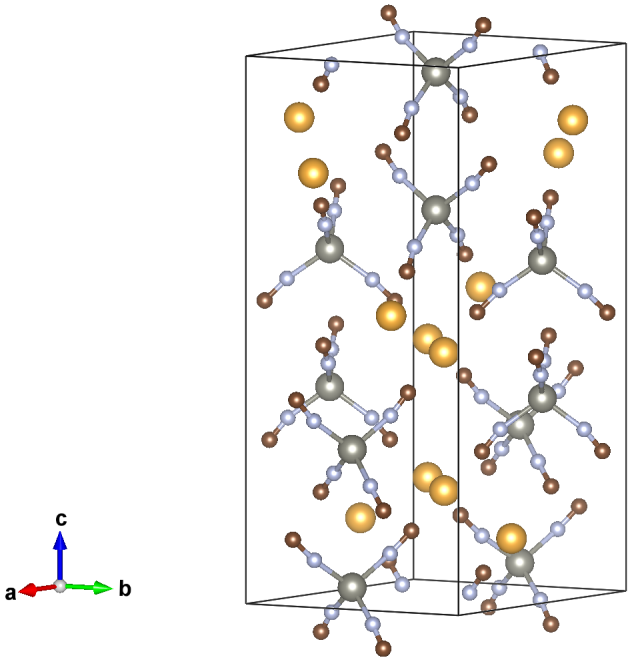

Figure 1: Unit cell structure of Zn-DAu material. It stabilizes in P6222 space group and lacks of K^+ ions. Zn atoms stabilize with a tetrahedral geometry. Structure taken from CCDC database[**?**].

1.2 Infrared spectroscopy

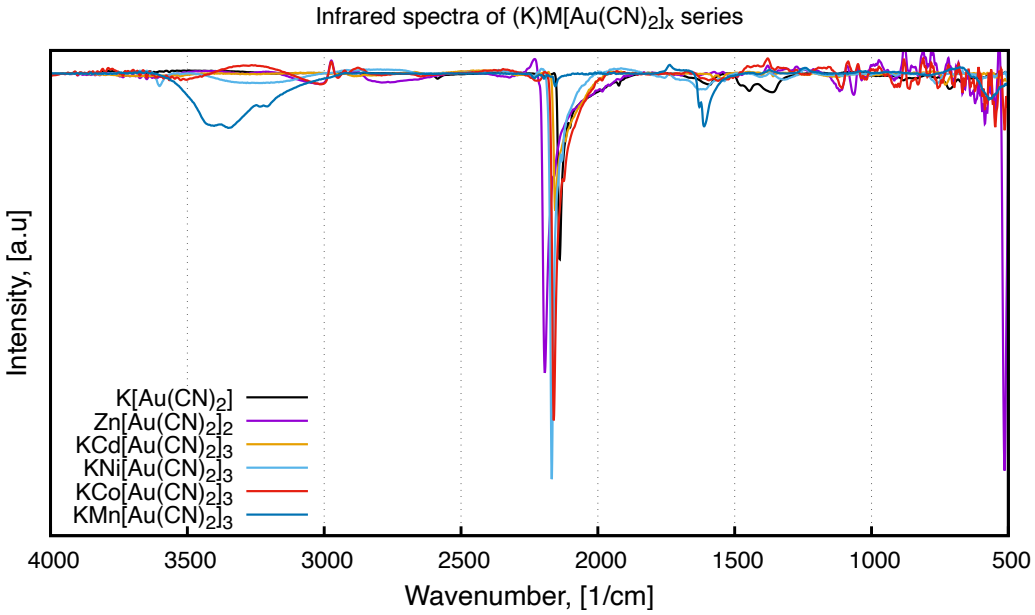

Figure 2: Infrared spectra of M-DAu materials.

1.3 Raman spectroscopy

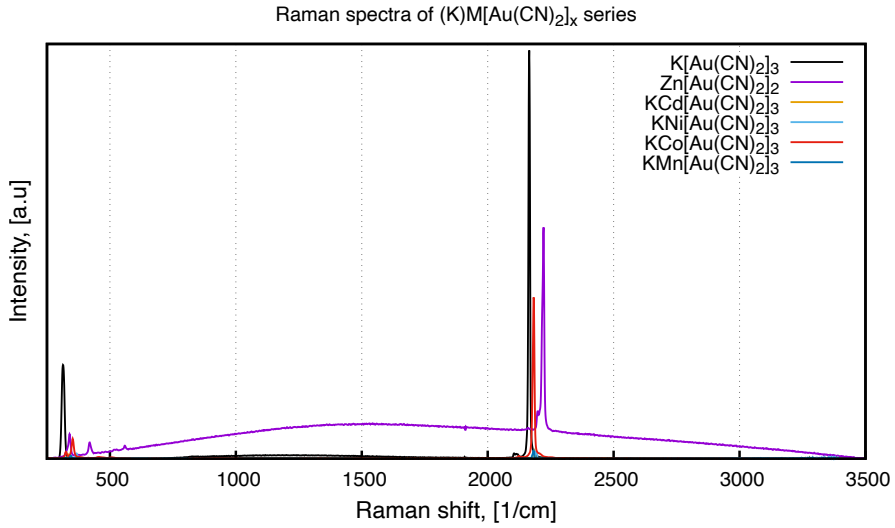

Figure 3: Raman spectra of M-DAu materials.

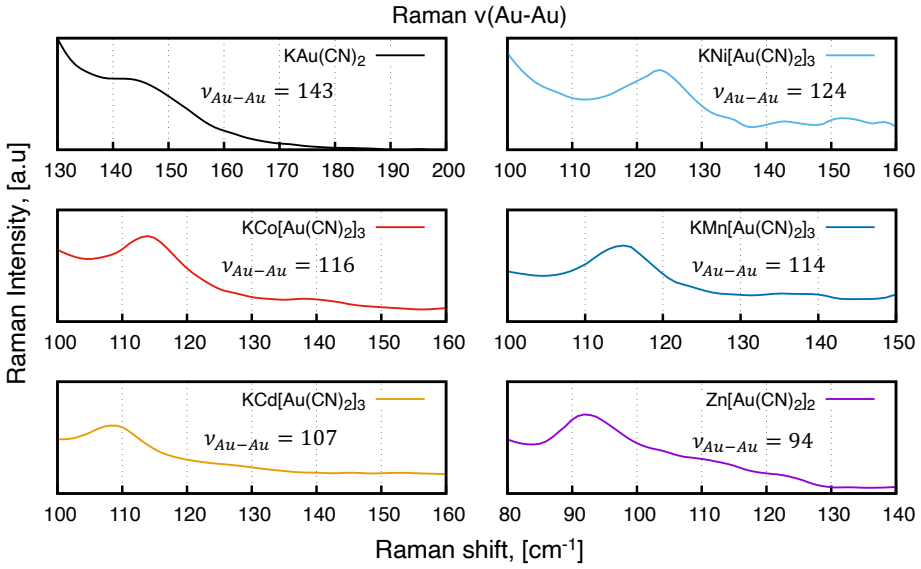

Figure 4: Aurophilic Au-Au stretching in the Raman low energy range.

1.4 Electronic spectroscopy and Tauc plots

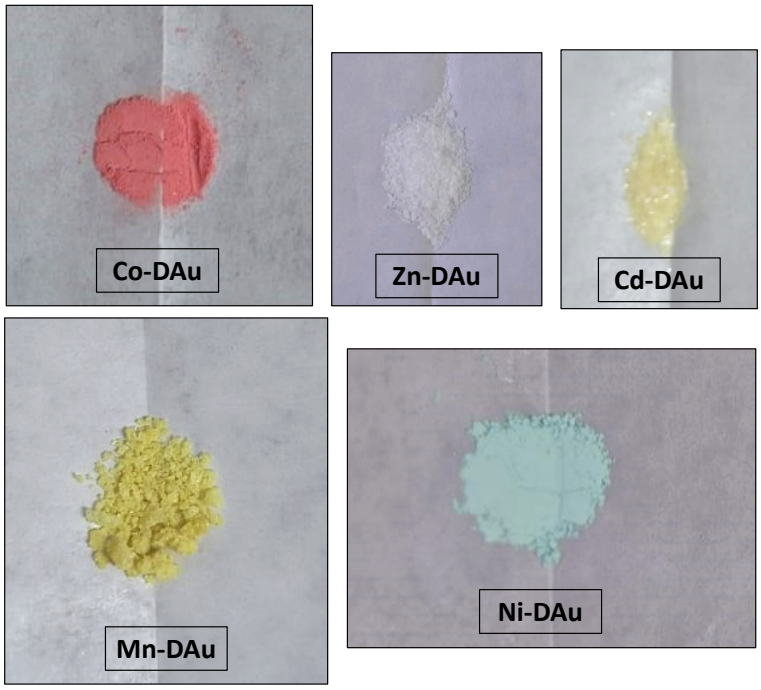

Figure 5: Synthesized M-DAu solids (M=Ni, Cd, Co, Zn and Mn). According to the semiconductor theory, the observed colors agree with the indirect transitions energy values obtained from Tauc analysis (Table 1).

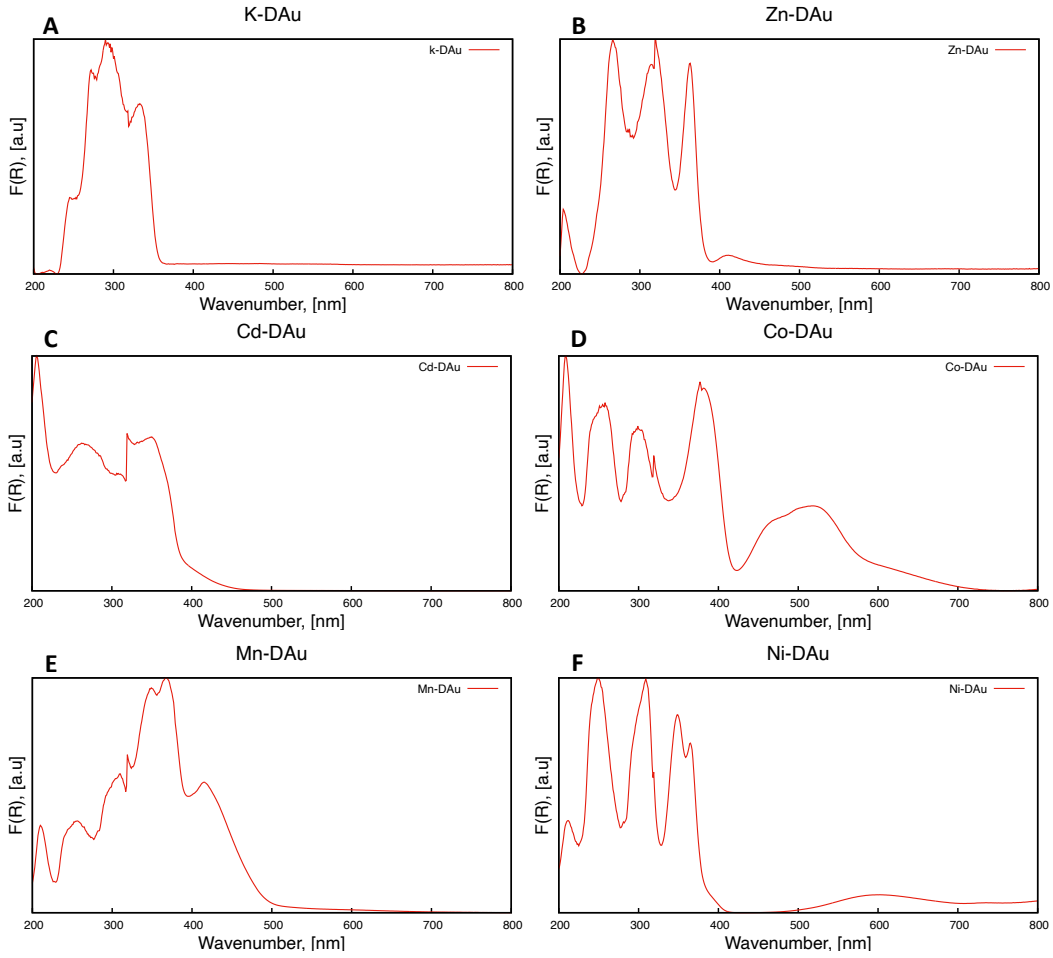

Figure 6: Absorption coefficient curves F(R) obtained from diffuse reflectance data (UV-Vis spectroscopy) of A. K-DAu, B. Zn-DAu, C. Cd-DAu, D. Co-DAu, E. Mn-DAu and F. Ni-DAu.

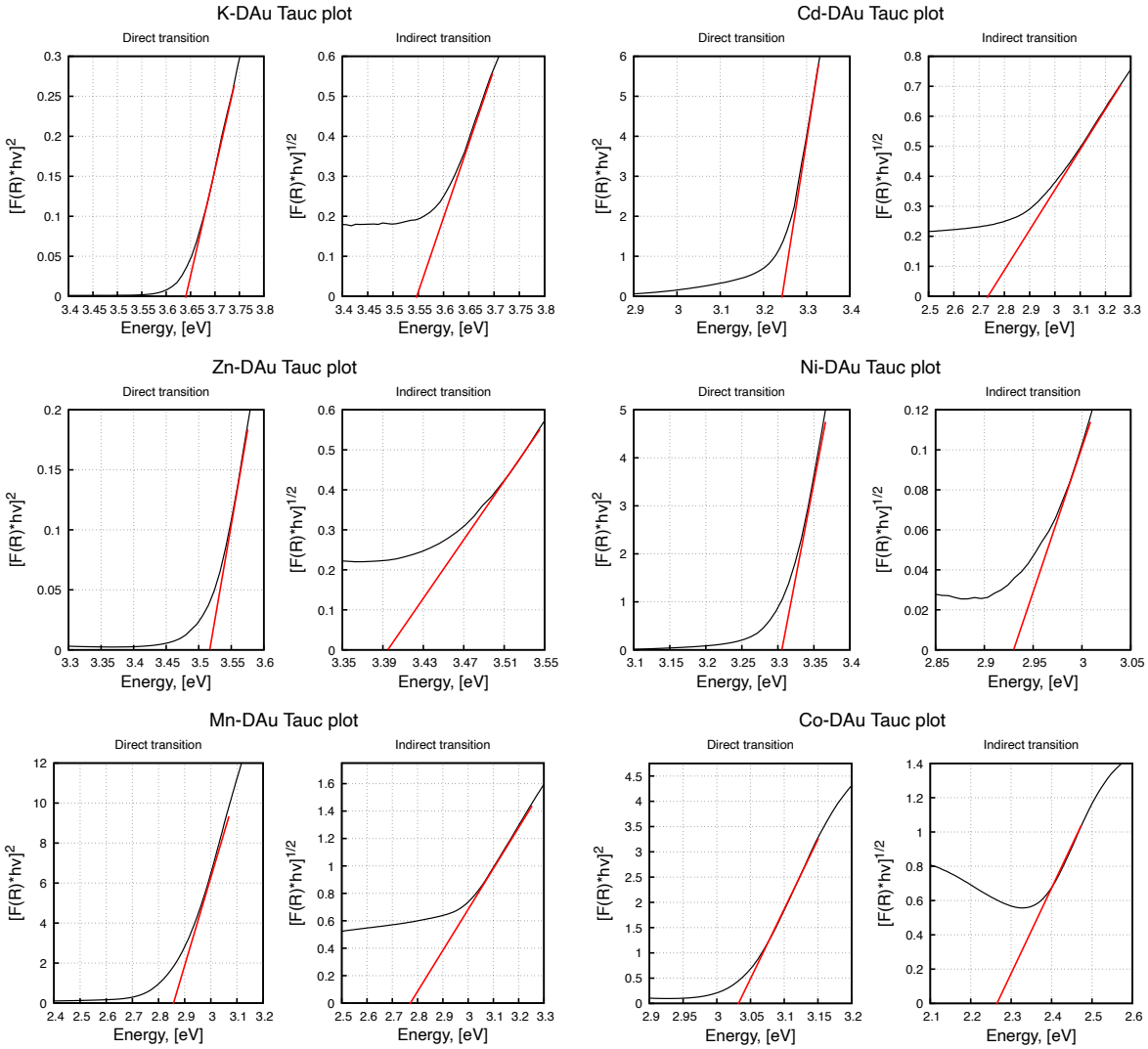

Figure 7: Tauc plotting of M-DAu materials. Allowed direct transitions (right) and allowed indirect transitions (left) are depicted. The obtained energies are summarized in Table 1.

2 Computational data

Simulated Lattice Parameters.						
System	F_{XC}	a(Å)	b(Å)	c(Å)	Volume(Å^3)	Au-Au(Å)
Co-DAu	HSE06	6.83	6.83	7.82	315.39	3.32
	PBE	6.79	6.79	7.80	311.43	3.31
Ni-DAu	HSE06	6.84	6.84	7.70	311.98	3.33
	PBE	6.81	6.81	7.70	309.25	3.30
Cd-DAu	HSE06	6.87	6.87	8.19	334.76	3.15
	PBE	6.82	6.82	8.27	333.12	3.17
Mn-DAu	HSE06	6.88	6.88	7.98	327.12	3.25
	PBE	6.81	6.81	8.31	333.75	3.21
Zn-DAu	HSE06	8.45	8.45	20.98	1297.33	3.15/3.11
	PBE	8.37	8.37	21.05	1277.13	3.11/3.02
K-DAu	HSE06	7.29	7.29	26.31	1210.90	3.61
	PBE	7.18	7.18	26.45	1180.88	3.35

Table 2: Lattice parameters of optimized structures. It is presented the results from HSE06 and PBE calculations.

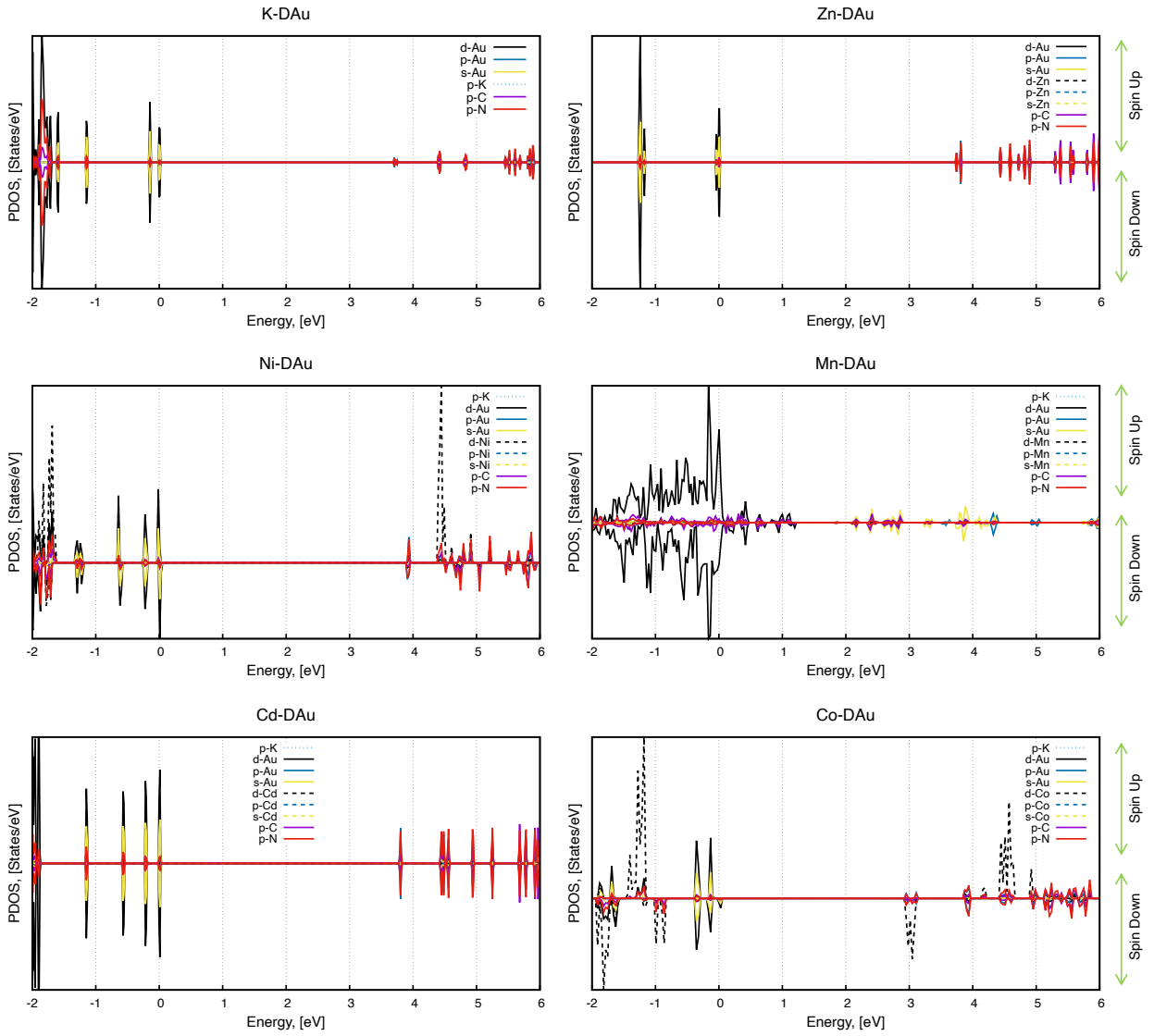

Figure 8: Orbital projected density of states (PDOS) of M-DAu materials (M=Zn, Cd, Ni, Co and Mn). PDOS data was obtained from spin-polarized calculations at hybrid HSE06 theory level. For simplicity, Fermi level was set to zero. No contributions of potassium (p-K) are observed.

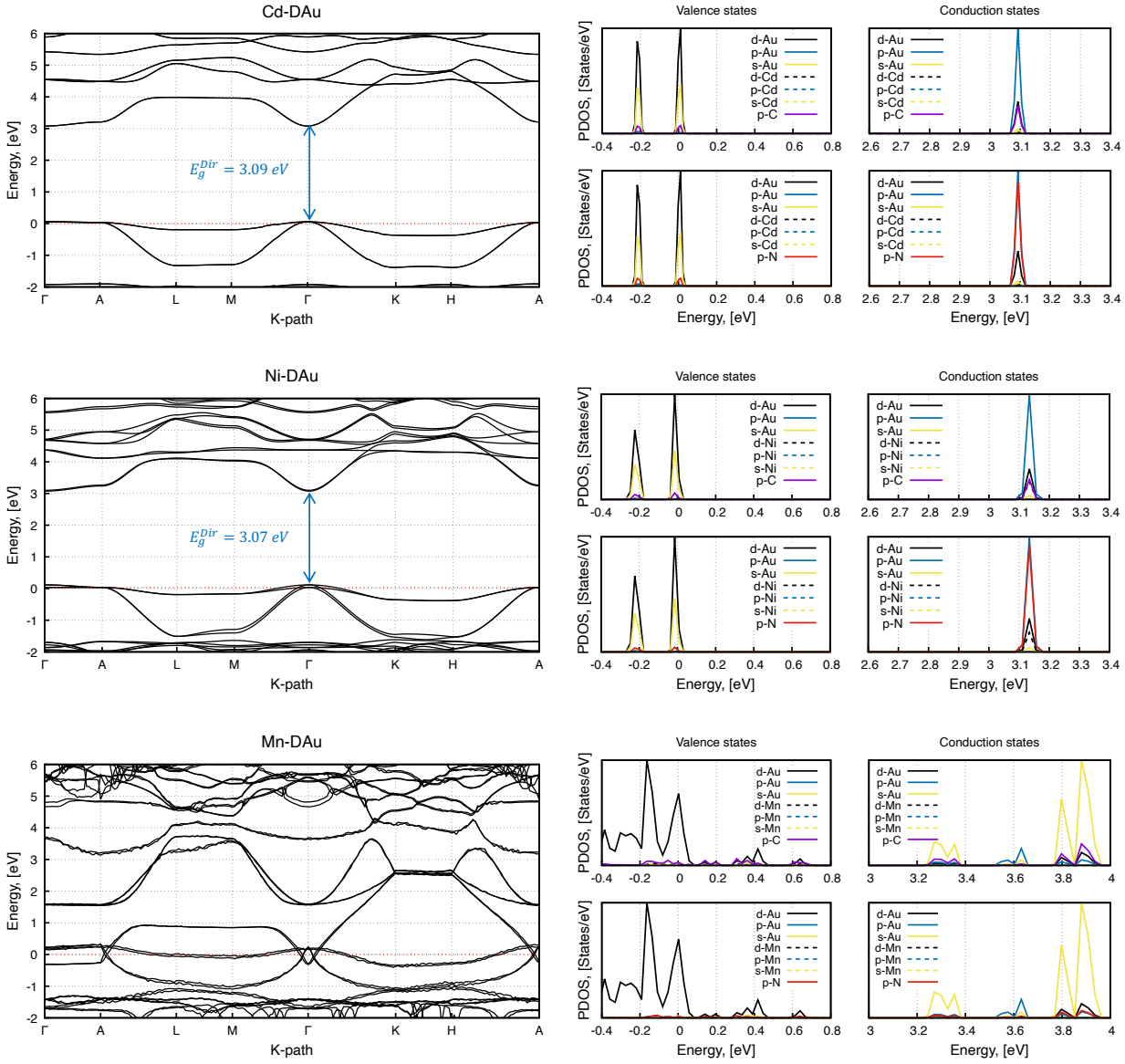

Figure 9: Band dispersion diagrams (left column) and projected density of states (right column) in the valence and conduction energy ranges of Cd-DAu, Ni-DAu and Mn-DAu. Band dispersion diagrams are potted along the $\Gamma \rightarrow A \rightarrow L \rightarrow M \rightarrow \Gamma \rightarrow K \rightarrow H \rightarrow A$ k-path for all the cases. Computations were carried out in the Brillouin space.

3 TEM images

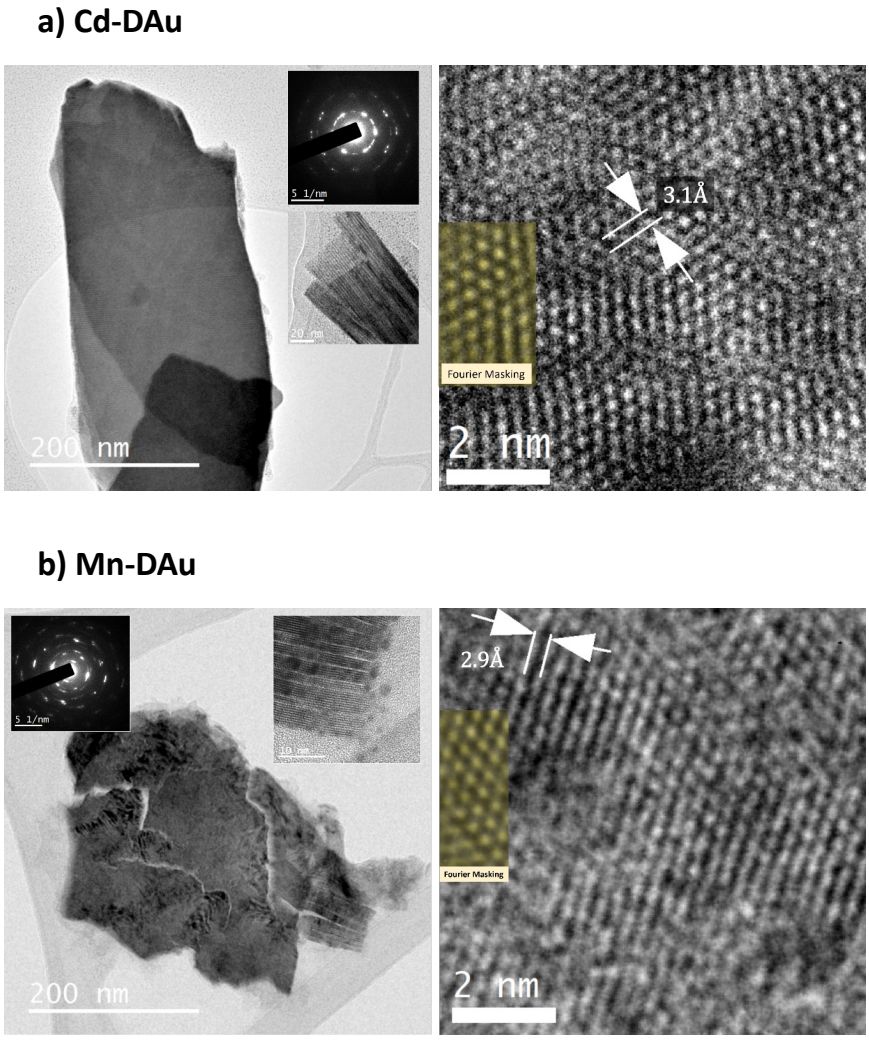

Figure 10: Images of Cd-DAu and Mn-DAu materials by BF-TEM depict the compounds has a lamellar thin morphology, and highly crystalline as shown by SAED pattern on the insert. Also, it is shown typical morphology of nanoribbons, from where HRTEM images were acquired and post processed by Fourier Masking (see yellow colored area) in order to determine interplanar distances which corresponds to crystalline planes ($\bar{1}$ $\bar{1}$ 1) 3.1 Å on Cd-DAu sample, and to crystalline planes (2 0 0) 2.9 Å on Mn-DAu sample, both in agreement with isomorphic compound KCo(Au(CN)2)3 ICSD 01-084-269 chart.

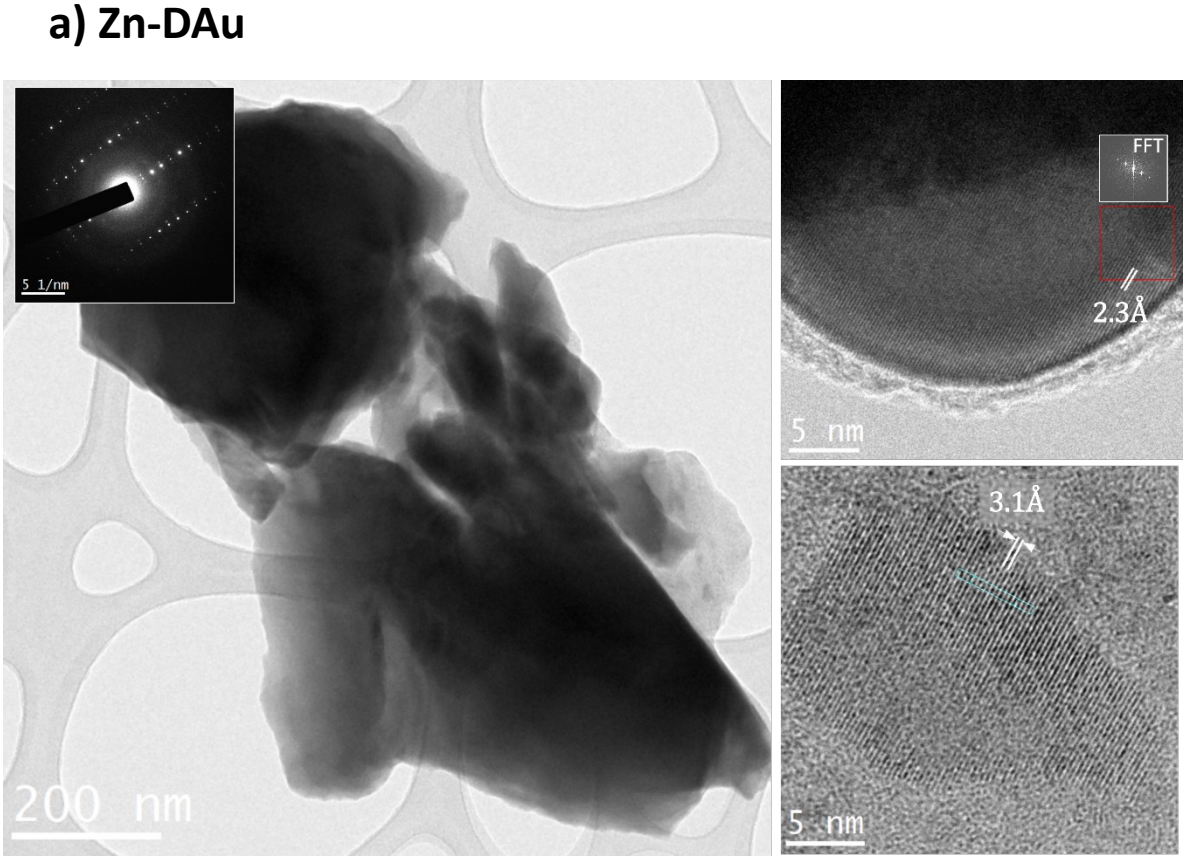

Figure 11: BF-TEM images of Zn-DAu sample depict bulky and thicker crystalline materials as shown by SAED pattern on the insert. Interplanar distances of 3.1 Å measured on segregated thin crystalline particles form HRTEM images, corresponds to crystalline plane ($\bar{1}$ $\bar{1}$ 1). Also, it is shown interplanar distance of 2.3 Å on bulky particles which corresponds to crystalline plane (2 0 2).

4 XRD patterns and structural data of Cd-DAu and Mn-DAu

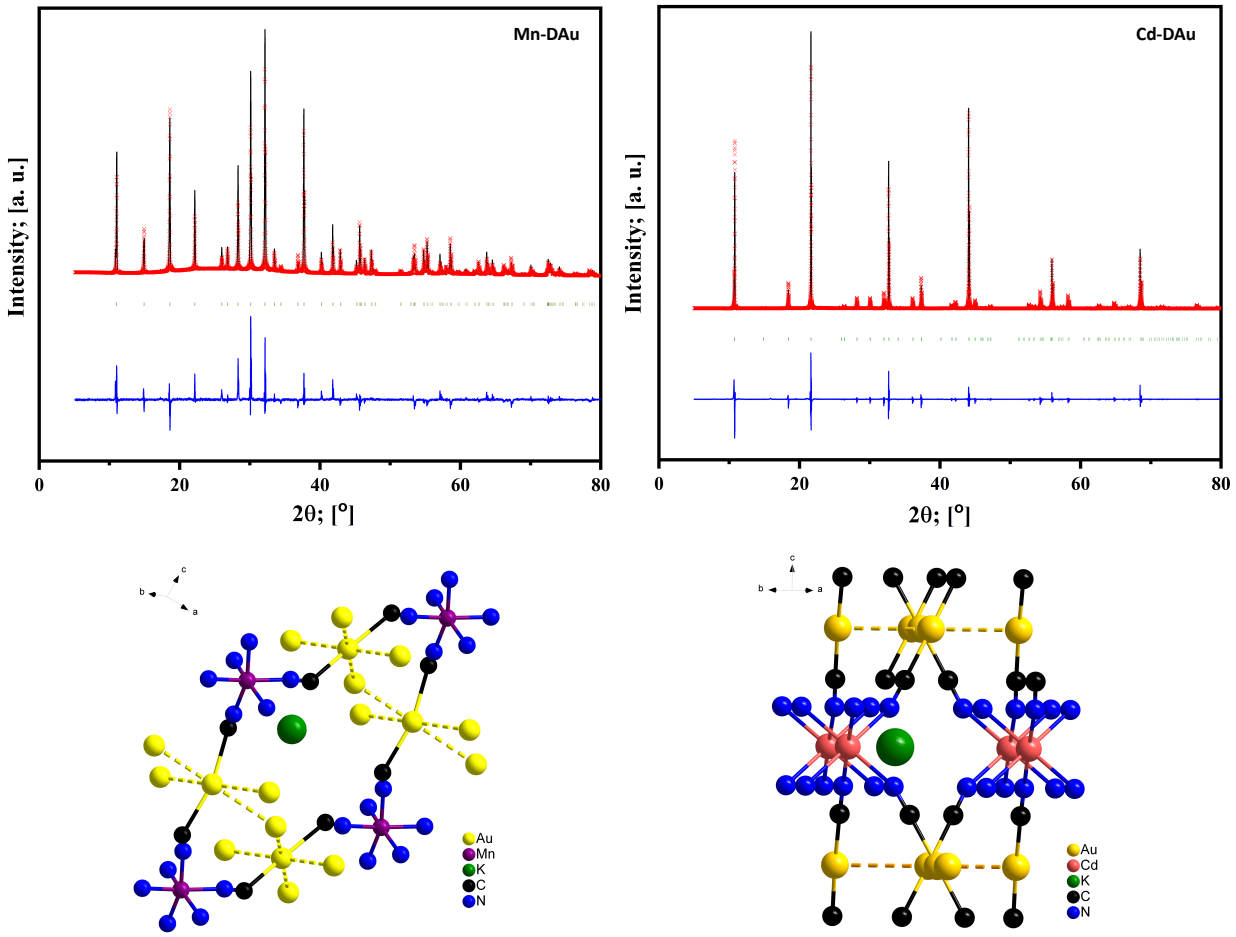

Figure 12: X-Ray difracction patterns and structural features of Mn-DAu (right) and Cd-DAu (left).

5 X-Ray Photoelectron Spetroscopy (XPS)

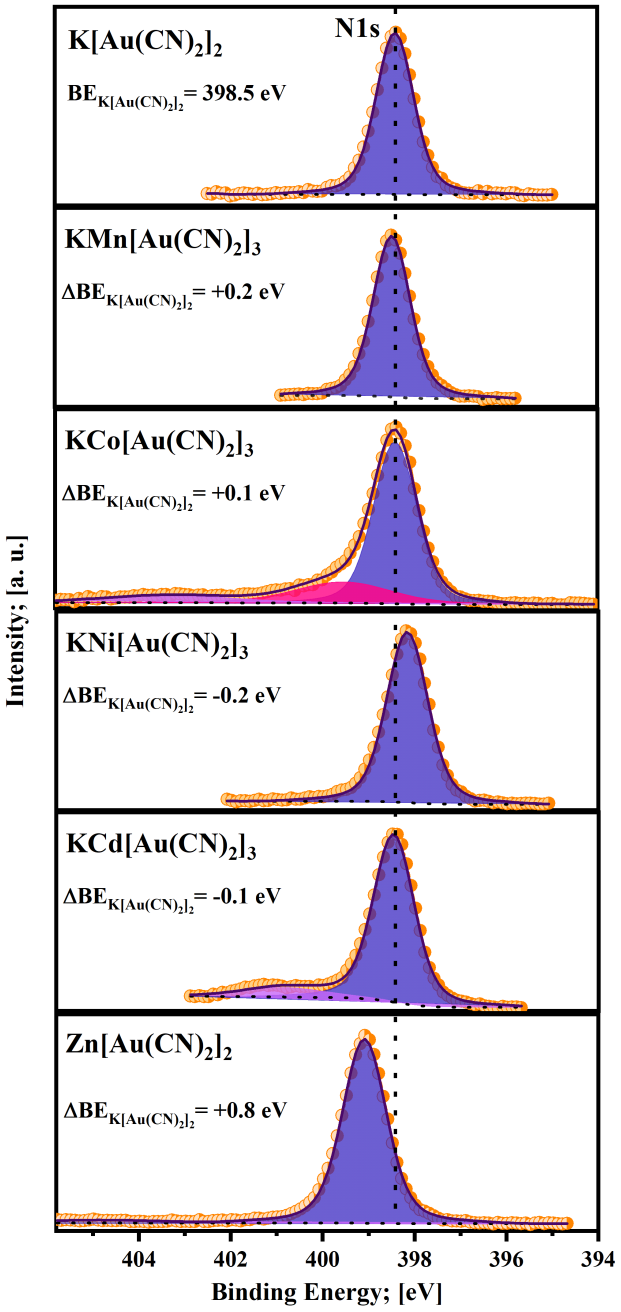

Figure 13: N1s signal X-Ray photoelectron spectra of the studied materials.

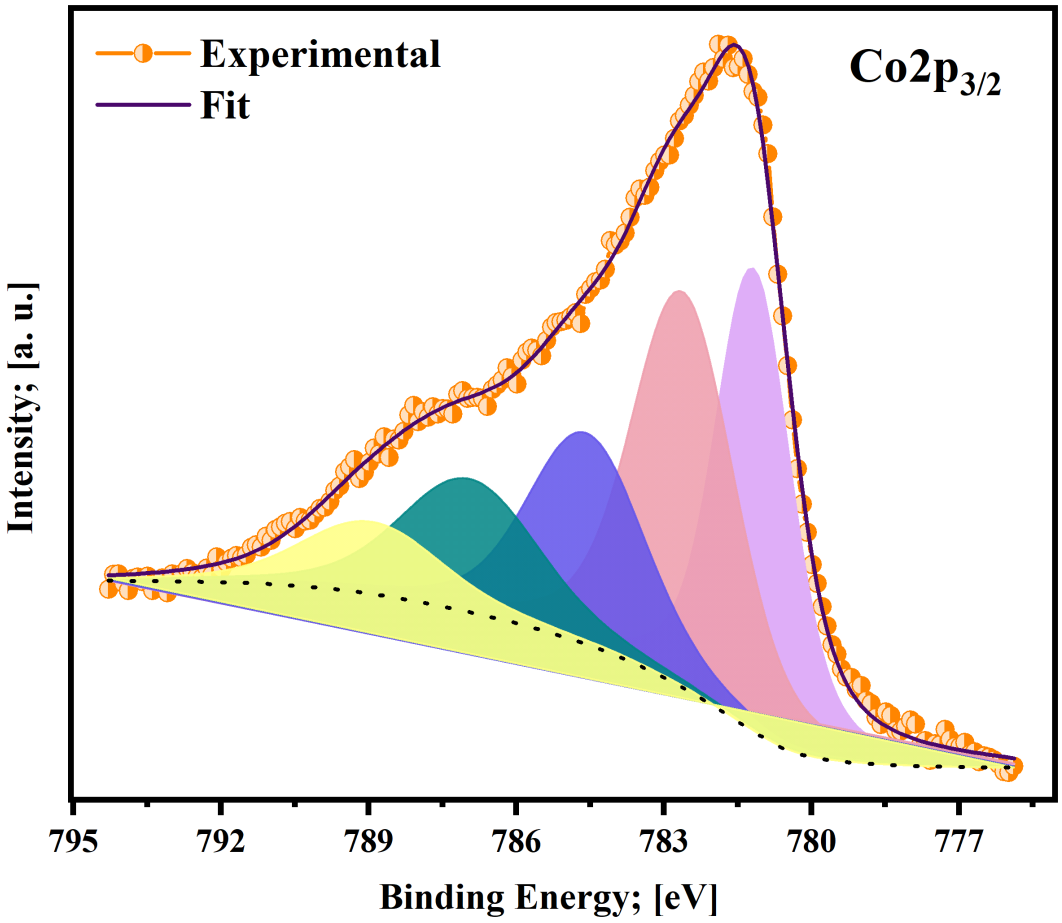

Figure 14: Auger signals of Co-DAu XPS spectrum.